PROCEEDINGS OF SCIENCE

Jets plus γ/Z in ATLAS

Benedetto Giacobbe* **on behalf of the ATLAS Collaboration**
Istituto Nazionale di Fisica Nucleare, Sezione di Bologna
E-mail: giacobbe@bo.infn.it

Recent measurements performed by ATLAS involving the associated production of jets with prompt photons or Z bosons in proton-proton collisions at $\sqrt{s} = 13$ TeV at LHC are presented. Differential cross-section measurements of such processes with respect to several kinematic variables and in different phase-space regions are used to probe both the QCD and EW sectors of the interactions. Experimental results are compared to state-of-art calculations and Monte Carlo simulations.

PoS(LHCP2018)195

Sixth Annual Conference on Large Hadron Collider Physics (LHCP2018)
4-9 June 2018
Bologna, Italy

*Speaker.

1. Introduction

Electroweak (EW) mediators such as the photon or the Z boson can be used to probe the Quantum Chromodynamics (QCD) sector of the proton-proton interaction when observed in association with jets in a cleaner environment with respect to the incusive jet production. Prompt photons are produced at LHC in the p-p hard-scatter through a direct interaction with the quarks, being therefore excellent probes of perturbative QCD (pQCD) and helping constrain the parton distribution functions. Their production cross-section is relatively large and, being colorless, they do not undergo hadronization, thus providing a clean and copious signal sample for precision measurements. The main bakground to prompt photons is due to neutral hadrons populating jets and decaying into photons, and can be suppressed with ad-hoc isolation cuts. At leading-order (LO), the prompt photon production with jets can proceed via two t-channel processes: *i)* direct ($qg \rightarrow q\gamma$) and *ii)* through the fragmentation of a colored parton. The relative importance of the two can be determined by measuring the distribution of the photon-jet scattering angle in the center-of-mass frame (θ^*) which depends on the spin of the mediator, a quark (gluon) in the first (second) case. Measurements involving prompt photons plus jets are also important to test the data description by the parton-shower generators in the high-energy regime, and to validate the Monte Carlo (MC) generators used to describe the background in searches beyond the Standard Model (BSM). The Z boson production is association with jets is dominated by the strong interaction, while dedicated phase spaces can be investigated in order to enhance the EW contribution. Z+jets events are copiously produced at LHC and experimentally clean to identify thanks to the leptonic decay of the Z boson, allowing precise measurements of differential cross-sections with respect to several kinematic and topological variables. In particular, the study of the jet multiplicity and kinematic properties and of the correlation between the jets are powerful tools for pQCD tests and for the modeling of the background in Higgs studies and new physics searches, of which Z+jets represents an important and irreducible background. Finally, the pure EW contribution to the associated production of Z plus jets represents a standard candle for other vector-boson fusion processes at the LHC, such as the Higgs boson production. In this document recent mesurements performed by ATLAS [1] in p-p collisions at $\sqrt{s} = 13$ TeV at LHC involving vector bosons and jets are discussed.

PoS(LHCP2018)195

2. Prompt-photons in association with jets

The measurement [2] was performed using the first collisions at $\sqrt{s} = 13$ TeV for a total luminosity of 3.16 ± 0.07 fb^{-1}. Photons are reconstructed in the region $|\eta| < 2.37$ starting from fixed-size sliding-window clusters in the electromagnetic calorimeter, and identified using the shower shapes in both the electromagnetic and hadronic calorimeters [3]. An isolation requirement is applied in order to remove the photons within jets: the energy deposited in the calorimeter in a cone of radius $\Delta R = 0.4$ around the photon (E_T^{iso}) is required to be $E_T^{iso} < 0.0042 \cdot E_T^{\gamma} + 4.8$ GeV, being E_T^{γ} the photon energy. Jets are reconstructed in ATLAS starting from topological clusters in both the hadronic and the electromagnetic calorimeters with an anti-k_T algorithm with parameter 0.4, followed by a multistep procedure based on a vertex-pointing correction, a pile-up and an underlying event subtraction and a multi-stage calibration based on MC and data and exploiting also the information from the tracking and muon systems [4]. The highest-p_T (leading) jet is required to have $p_T^{jet} > 100$ GeV and rapidity $|y^{jet}| < 2.37$, and events with one such jet and one photon with $E_T^{\gamma} > 125$ GeV are retained. Other jets are required to have $p_T^{jet} > 60$ GeV in the same rapidity region. For the measurements of the photon-jet invariant mass $m^{\gamma-jet}$ and of $cos(\theta^*)$ the additional constraints $|\eta^{\gamma} + y^{jet-lead}| < 2.37$, $|cos(\theta^*)| < 0.83$ and $m^{\gamma-jet} > 450$ GeV are used to remove the bias due to the photon and jet selection requirements. The differential cross-section measurements are affected by a systematic uncertainty ranging from 4 to 10%, dominated by the jet and photon energy scales and the photon identification. The measured differential cross-sections as a function of E_T^{γ} and p_T^{jet} are shown in figure 1 and compared to the LO-predictions by PYTHIA and SHERPA. The shape of E_T^{γ} is well described over a range of almost 6 orders of magnitude by both models, while PYTHIA overstimates the p_T^{jet} distribution above ~ 200 GeV due to large constribution from photon bremsstrahlung predicted by PYTHIA. In figure 1 the scattering angle distribution is also shown compared to the LO JetPhox predicted cross-sections for direct and fragmentation processes: the measured distribution is consistent with the dominance of the direct production. In figure 2, the measured differential cross-sections with respect to p_T^{jet}, to the angular distance between the photon and the leading-jet ($\Delta\Phi^{\gamma-jet}$) and $m^{\gamma-jet}$ are shown, compared to NLO predictions by SHERPA and JetPhox. In general, both calculations provide a good descritpion of the data within the theoretical and experimental uncertainties ($\Delta\Phi^{\gamma-jet}$ can only be reliably predicted by SHERPA due to the inclusion of the processes $\gamma + 1, 2$ jets at NLO and $\gamma + 3, 4$ jets at LO additional to its parton shower). It is important to note that the experimental uncertainties are smaller than the theoretical ones. The total fiducial cross-section is measured to be $\sigma_{fid} = 300 \pm 10(exp) \pm 6(lumi)$ pb, consistent with the SHERPA and JetPhox NLO calculations.

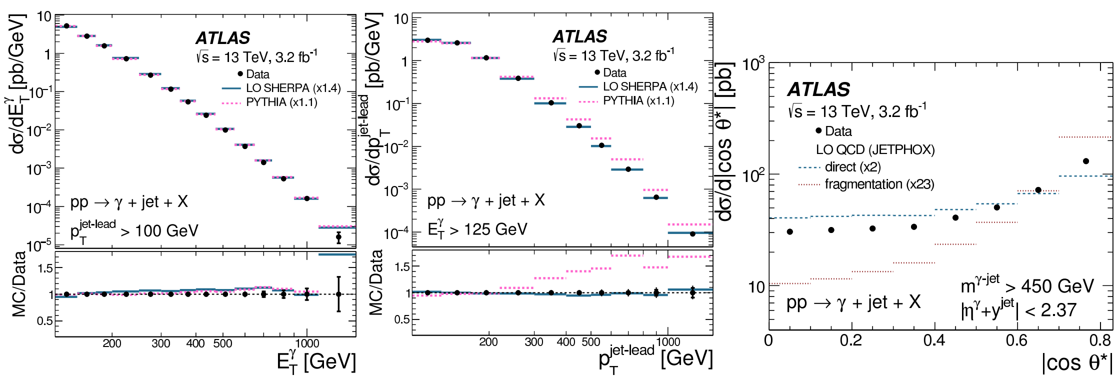

Figure 1: Measured cross-sections as a function of E_T^{γ} (left) and p_T^{jet} (center) compared to SHERPA and PYTHIA predictions at LO. Right: Measured cross-section as a function of $cos(\theta^*)$ compared to LO predictions by JetPhox normalized to the integrated cross-section. Distributions use leading photon and jet [2].

3. Z boson in association with jets

The measurement [5] is performed using the same data sample of the analysis discussed above. Differential cross-sections are measured with respect to several variables such as the jet multiplicity, the leading-jet p_T^{jet} and rapidity (y^{jet}), the scalar p_T sum of all final-state objects in the event (H_T), the jet-jet angular distance ($\Delta\Phi_{jj}$) and mass (m_{jj}). The Z boson is defined as two opposite-

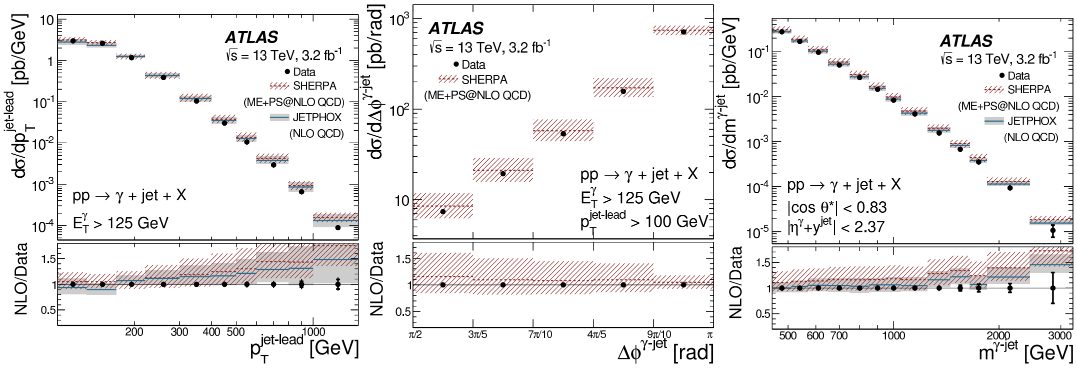

Figure 2: Measured cross-sections as a function of P_T^{γ} (left), $\Delta Phi^{\gamma-jet}$ (center) and $m^{\gamma-jet}$ (right) compared to NLO SHERPA and JetPhox predictions. Distributions use the leading photon and leading jet [2].

charge same-flavour leptons (electrons or muons) with invariant mass $71 < m_{ll} < 111$ GeV. Electrons are required to have $p_T > 25$ GeV, $|\eta| < 2.47$ excluding the barrel-endcap transition region $1.37 < |\eta| < 1.52$, and fulfill medium-quality identification requirements [6]. Muons with $p_T > 25$ GeV, $|\eta| < 2.4$ and medium-quality identification requirements [7] are retained. Both leptons must fulfill p_T-dependent isolation requirements. Jets are reconstructed as described above and are required to have $p_T > 30$ GeV and $|y| < 2.5$ and not to overlap with the leptons. Backgrounds are estimated via MC (EW and top) or with a data-driven techique (multijet). Data distributions are unfolded to the particle level using a Bayesian technique [8] to take into account and correct for detector inefficiencies, resolutions and systematic biases. The muon and electron channels are combined in order to improve the precision of the measurement by taking into account the correlation of the systematic uncertainties. The measured cross-sections are compared to the fixed-order calculations at next-to-leading order (NLO) from BlackHat+SHERPA and at next-to-next-to-leading order (NNLO) from the $Z+\geq 1$ jet Njetti calculation, and to predictions from the MC generators SHERPA 2.2, Alpgen+Py6, MC_aMC+Py8 CKKWL and MG5_aMC+Py8 FxFx. In figure 3 the measured cross-section is shown as a function of the inclusive jet multiplicity (left) and of the ratios of the successive inclusive jet multiplicities (right). The generator predictions, normalised to the inclusive NNLO cross-sections, are superimposed and they are in agreement with data except for SHERPA 2.2, Alpgen+Py6 and MG5_aMC+Py8 FxFx for high jet multiplicity, where a non negligible fraction of the jets are produced by the parton shower. In figure 4 the measured cross-sections as a function of p_T^{jet} (left), H_T (center) and $\Delta\Phi_{jj}$ (right) are shown. p_T^{jet} is a sensitive probe of the pQCD understanding over a large range and a crucial variable to model the background for Standard Model and BSM studies. The predictions are in agreement with the data within the uncertainties, with the exception of MC_aMC+Py8 CKKWL which models a too hard spectrum. H_T is a variable used to observe final states from BSM heavy particles decays. While SHERPA 2.2, Alpgen+ Py6 and MG5_aMC+Py8 FxFx well describe the data, MG5_aMC+Py8 CKKWL description is not satisfactory at high H_T consistent with the poor description of the high-p_T spectrum. The fixed-order prediction from Black-Hat+SHERPA underestimates the cross-section for $H_T > 300$ GeV because of the missing contributions from events with higher parton multiplicities, the agreement being improved by adding higher orders pQCD terms as in Njetti. $\Delta\Phi_{jj}$, a useful variable for separating Z+jets from heavier particles, is well described by all predictions.

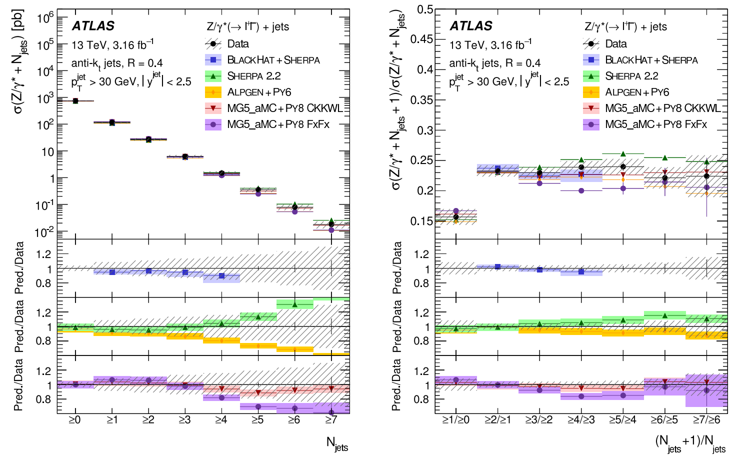

Figure 3: Measured particle-level cross-section as a function of the inclusive jet multiplicity (left) and of the ratios of the successive inclusive jet multiplicities (right). Predictions from various generators are superimposed in the top panels. In the bottom panels the prediction-to-data ratios are shown [5].

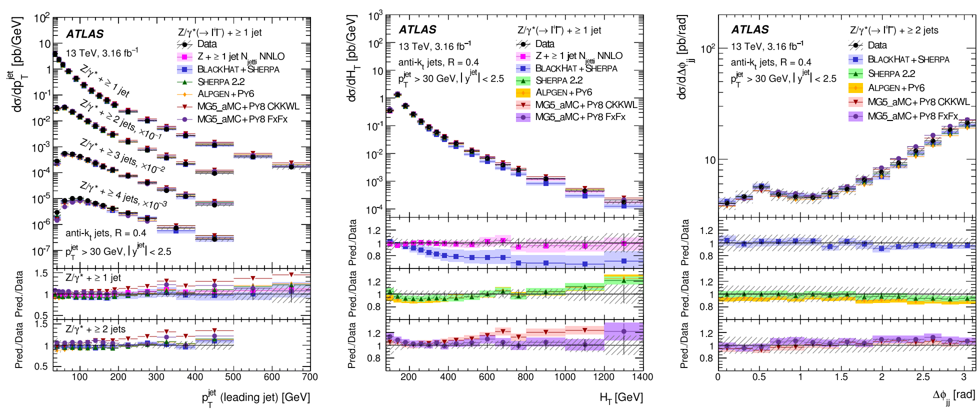

Figure 4: Measured cross-section as a function of the p_T of the leading jet for $Z+\geq 1,2,3,4$ jets (left), H_T for $Z+\geq 1$ jet (center) and $\Delta\Phi_{jj}$ for $Z+\geq 2$ jets (right). The predictions of the used generators are shown and the prediction-to-data ratios are reported in the lower panels [5].

4. EW Z boson production in association with di-jets

The production of the Z boson in association with jets is dominated by QCD mechanisms, with smaller contributions from vector-boson fusion EW processes, where the absence of colour connection between the two quarks implies a smaller probability for additional jets to be produced in the rapidity interval between the two leading jets with respect to the QCD production. EW Zjj events are therefore characterized by two high-energy jets separated by a large rapidity gap and with large dijet mass (m_{jj}). Moreover, a p_T balance between the Z boson and the dijet system is present, while in the QCD-mediated production the balance involves also the additional jet in the rapidity gap. Several phase-space regions are therefore built [9] with an increasing purity of the EW component: from a QCD-enriched region (requiring additional jets in the rapidity gap and p_T balance between the three leading jets and the Z) to an EW-enriched (with no hadronic activity in the rapidity gap and a p_T balance between the two leading jets and the Z) to a further EW-enriched with the additional requirement $m_{jj} > 1$ TeV, with estimated EW-purities of $< 2\%$, $\sim 5\%$ and $\sim 26\%$, respectively. In order to measure the EW cross-section it is crucial to correctly estimate the remaining QCD background. In figure 5, the QCD-enriched m_{jj} spectrum, used as a control region (CR) for the EW-enriched background, is shown. A negligible EW component is visible as expected, but the description of the QCD spectrum provided by SHERPA (and by other generators) is poor. A data-driven shape correction to the predicted m_{jj} spectrum is applied by using the data-to-MC ratio in the CR and is shown in figure 5 (center) as obtained with different generators. After the mismodeling correction a very satisfactory data-to-predictions agreement is obtained as shown in figure 5 (right), where the EW-enriched m_{jj} spectrum is represented as a composition of the EW signal and the QCD background. As expected, the EW component increases at large mass. In figure 6 (left) the EW Zjj cross-section is represented for the EW-enriched and high-mass regions both at 8 TeV [10] and 13 TeV, showing an increase by factors 2.2 and 3.2 respectively, well described by POWHEG. In figure 6 (right), the Zjj fiducial cross-sections measured by ATLAS both at 8 and 13 TeV are reported for all the phase-space regions, together with the theoretical predictions provided by various combinations of generators.

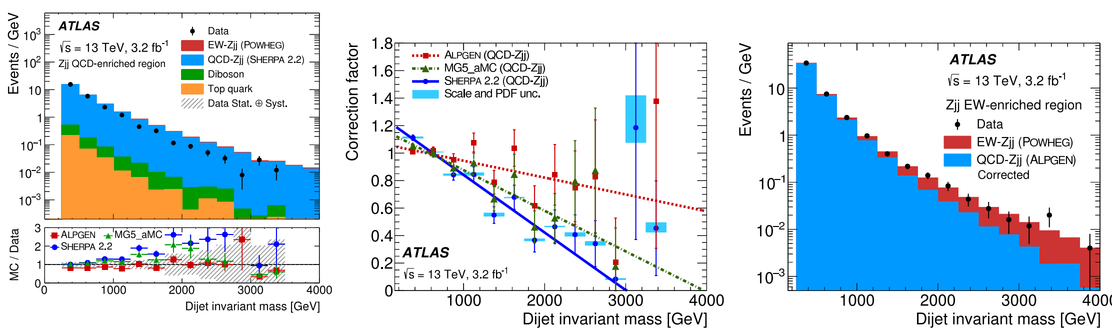

Figure 5: Dijet invariant mass distribution in the QCD-enriched region compared to simulation (left). Data-to-simulation ratio shape correction factors with different QCD Zjj generators (center). Dijet invariant mass distribution in the EW-enriched region after correction of the QCD Zjj template to the data (right) [9].

5. Conclusions

Processes involving the associated production of vector bosons with jets in pp collisions at the LHC are a powerful tool to test the pQCD at very high energy. Precise measurements in this sector can help to validate the MC generators and to model some of the main backgrounds in Higgs and BSM studies. ATLAS has performed a wide set of measurements in this field also thanks to the excellent performance in photon and jet reconstruction which usually represent the dominant sources

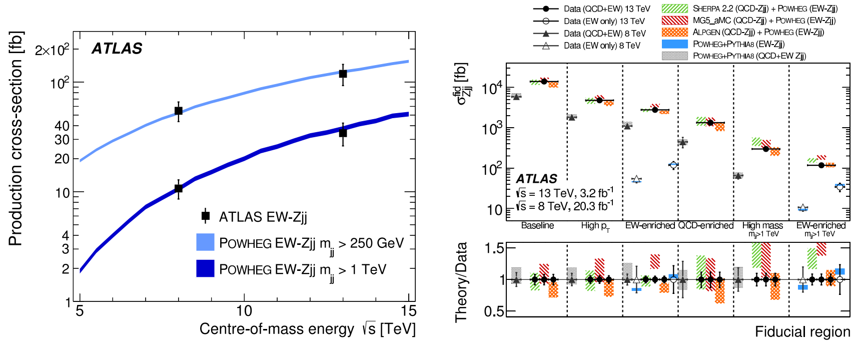

Figure 6: Zjj cross-sections in the EW-enriched and high-mass regions as measured by ATLAS at 8 and 13 TeV center-of-mass (left). Fiducial cross-sections of Zjj (both QCD+EW and EW only) measured by ATLAS at 8 and 13 TeV compared to various QCD and EW prediction combinations [9].

of systematic uncertainties. The measurements are more precise than the theoretical predictions, implying that improvements in the calculations will make it possible to use the data to discriminate among models. Other analyses using data at 13 TeV are ongoing and will soon converge.

References

[1] ATLAS Collaboration,"The ATLAS experiment at the CERN large hadron collider", J. Inst. 3 (2008) S08003.

[2] ATLAS Collaboration,"Measurement of the cross-section for isolated-photon plus jet production in pp collisions at $\sqrt{s} = 13$ TeV using the ATLAS detector", Phys. Lett. B780 (2018) 578.

[3] ATLAS Collaboration,"Electron and photon energy calibration with the ATLAS detector using LHC Run1 data", Eur.Phys.J. C74 (2014) 3071. ATLAS Collaboration,"Measurement of photon identification efficiencies with ATLAS detector using LHC Run1 data", Eur. Phys. J. C76 (2016) 666

[4] ATLAS Collaboration,"Jet energy scale measurements and their systematic uncertainties in proton-proton collisions at $\sqrt{s} = 13$ TeV with the ATLAS detector", Phys. Rev. D96 (2017) 072002

[5] ATLAS Collaboration,"Measurements of the production cross section of a Z boson in association with jets in pp collisions at $\sqrt{s} = 13$ TeV with the ATLAS detector", Eur. Phys. J. C77 (2017) 361.

[6] ATLAS Collaboration,"Electron efficiency measurements with the ATLAS detector using the 2015 LHC proton-proton collision data", ATLAS-CONF-2016-024. http://cdsweb.cern.ch/record/2157687

[7] ATLAS Collaboration,"Muon reconstruction performance of the ATLAS detector in proton proton collision data at $\sqrt{s} = 13$ TeV", Eur. Phys. J. C76 (2016) 292.

[8] G. D Agostini,"A multidimensional unfolding method based on Bayes theorem", Nucl. Instrum. Meth. A362 (1996) 487.

[9] ATLAS Collaboration,"Measurement of the cross-section for electroweak production of dijets in association with Z boson in pp collisions at $\sqrt{s} = 13$ TeV with the ATLAS detector", Phys. Lett. B775 (2017) 206.

[10] ATLAS Collaboration,"Measurement of the electroweak production of dijets in association with a Z boson and distributions sensitive to vector boson fusion in proton-proton collisions at $\sqrt{s} = 8$ TeV using the ATLAS detector", JHEP04 (2014) 031. arXiv:1401.7610.